II Congresso Aeroespacial Brasileiro

De 16 a 19 de setembro

EXPERIMENTAL STUDY OF THE INSULATING EFFECTIVENESS OF SILICONE RUBBER COMPOSITES BY OXYACETYLENE ABLATION TESTING

Artem Andrianov, Jungpyo Lee, Gabriela Possa, Hiterson de Oliveira Silva
Universidade de Brasília, Faculdade UnB Gama (FGA), Engenharia Aeroespacial, Área Especial de Indústria Projeção A, Setor Leste, Gama, CEP: 72444-240

Resume: *The objective of this study is to characterize the thermal insulation efficiency of silicone rubber reinforced composites by oxyacetylene torch. These composites reinforced by glass, carbon, ceramics and silica fibers are intended to be used as ablators in a low-thrust hybrid propulsion motor. The back-face temperature measurements are used as a criterion for insulation efficiency of the specimens, whose frontal face is subjected to oxyacetylene flame for 40 s. The paper includes the results of ablation rate measurements and the influence of orientation of glass and carbon fibers relatively to the flame direction on back-face temperature of the specimens.*

Keywords: *Thermal insulators, Ablation, Oxyacetylene torch, Silicone rubber.*

1. INTRODUCTION

The presented study was motivated by the necessity of a prolonged fire testing of the low thrust hybrid propulsion motor developed at the University of Brasilia (ANDRIANOV, 2015). The required operation time of the motor should be at least 40 seconds, what necessitates special measures to ensure thermal protection of the motor casing. Thermal protection for hybrids can be adopted from solid propellant rocket motors. In solid propulsion systems, it is realized by internal insulation, which functions as a heat barrier primarily through the mechanism of ablation (NASA, 1977). Generally, insulators for SRM are identified by filler (reinforcement) and matrix (binder); the latter identifies the class of insulation material, which can be thermosetting or elastomeric plastic (AHMED, 2009). The most common thermosetting matrix is phenolic resin, a char yielding material with good temperature resistance, but with relatively low elasticity, which limits its application for heat insulation of motor casings experiencing high deformations. Thus, body insulations are normally elastomeric composites conferring strain tolerance (YOUREN, 1971).

According to extensive literature review on elastomeric heat-shielding materials for rocketry (DONSKOY, 1996), the most appropriate elastomeric heat shielding matrices are nitrile-butadiene, ethylene-propylene and silicone organic rubbers. Fabrication of insulators from the first two elastomers requires a complex technological process including vulcanization at elevated temperatures. Sophisticated manufacturing process may affect the main advantages of a hybrid propulsion technology, such as flexibility and architecture simplicity (MAZETTI, 2016). At the same time, a wide range of organic silicones does not require complex technological process and can be vulcanized at room temperatures. According to data provided by (DONSKOY, 1996), erosion resistance for silicone elastomer filled with carbon (density 1.16 g/cm^3, ablation rate 0.020 mm/s) is slightly greater than for ethylene-propylene rubber filled with asbestos fiber (1.23 g/cm^3, 0.015 mm/s), polypropylene rubber filled with carbon (1.24 g/cm^3, 0.015 mm/s) and silica (1.45 g/cm^3, 0.019 mm/s).

The extensive literature review (NATALI, 2016) covers all necessary information on types, technology, testing techniques and application of ablative materials in the aerospace industry, including polysiloxanes (or silicones). According to the given review, silicones are effective matrices for thermal protections systems due to: 1) relatively low density 1 – 1.2 g/cm^3; 2) good thermal resistance (because of high binding energy of Si-O bond); 3) capability of yielding siliceous/carbonaceous char; 4) high oxidation resistance in comparison to

Primeiro Autor: andrianov@aerospace.unb.br

other char yielding polymers. Thermal resistance of silicones is supported by high binding energy of Si-C bond in comparison with C-C bond in the main chain of hydrocarbon elastomers, possibility to rearrange molecular structure under thermal influence and to form cyclic molecular compounds (DONSKOY, 1996). Polymers with rings in the polymer chain form a high percentage of char during pyrolysis, which improves erosion resistance of insulator (SCHMIDT, 1969). Besides that, a char layer is supported by a silicone backbone structure even in case when a char layer experiences severe conditions of pressure and temperatures up to 1000°C in the conditions of induced air combustion chamber (OYUMI, 1998). More detailed review for thermal degradation mechanism of polysiloxanes is given in reference (ZHOU, 2006).

It should be noted that high thermal insulation characteristics of silicone elastomers (such like a lower rate of ablation and higher insulation index tested in oxy-acetylene flame in comparison to other elastomers: butadiene acrylonitrile, chloroprene, urethane etc.) have been known for a long time (SCHMIDT, 1965).

At some conditions of heating, decomposition of silicone is slower than in phenolic resin (FAVALORO, 1998): at temperature 700°C the volatilized portion for silicone is near 20% and for phenolic resin is near 50%. As the experimental study (CHAPMAN, 1966) shows, the ablative material with a silicone resin base produced the highest performance in a moderate range of conditions (heat rate below 1.14 MW/m2 and dynamic pressure below 2.4 kN/m^2) provided by electric-arc-heated gas stream in comparison to phenolic and epoxy base materials. The tests (KOO, 2011; MILLER, 1994) with use of small-scale liquid-fueled rocket motor burning kerosene-oxygen showed that silicone is more thermally stable and more preferred polymer matrix than the phenolic resin for ablative components of vertical launch systems subjected to exhaust plume from solid rocket motors.

In the reference (YANG, 2013a) it was shown that in oxy-acetylene flame the silicone rubber filled with silica and carbon fibers yields the ablative layer, whose thermo-oxidative stability is better than that that of virgin material due to formation of silica, silicone carbide and aromatic carbon, which transforms into inorganic carbon. Ablative properties can be improved by reinforcement of silicone rubber with various inorganic fibers: not only carbon (KIM, 2008; KIM, 2011), but also silicone carbide (ZHANG, 2016), silicate ceramic (YU, 2014; ZHOU, 2015), zirconium carbide (YANG, 2013b) and others. However, the authors compare efficiency of reinforced composites with a virgin silicone rubber, and it is not clear how various types of fillers affect the insulating effectiveness of silicone composite.

According to the reference (DONSKOY, 1996), there are few information about rubbers reinforced with fabrics. The experimental data on insulating effectiveness for various types of fillers in silicone matrix and elevated heat fluxes are given in the reference (KOO, 2011). The objective of the presented study is to fill the data gap in the range of moderate heat fluxes, which are inherent to low-thrust hybrid propellant motors (NUNES, 2017). The back-face temperature measurements are used as a criterion for insulation efficiency of the silicone rubber specimens, whose frontal face is subjected to oxyacetylene flame for 40 s. The specimens were reinforced with four types of widely available fabrics and tapes based on glass, carbon, ceramics and silica fibers. Other objectives of the study are comparison of the mass ablation rate of silicone composites and evaluation of back-face temperature of the specimens with parallel and perpendicular orientation of glass and carbon fibers relatively to the oxyacetylene flame direction.

2. MATERIALS

The characteristics of silicone rubber composites reinforced by glass, carbon, ceramic and silica fibers with perpendicular and parallel orientation in relation to flame direction are given in Tables 1 and 2, respectively. The silicone rubber was obtained by combination of polydimethylsiloxanes with inorganic fillers (delivering conditions) and copper phthalocyanine. Polydimethylsiloxane was used as a matrix due to low cost and simple processing. Ablation characteristics of the silicone rubber in conditions of burning of liquid nitrous oxide and solid paraffin fuel grain (conditions of the low-thrust hybrid propellant rocket motor) are given in (MILHOMEM, 2017).

The specimens were manufactured by manual lay-up technology at room temperatures, and cut to dimensions of 50±1 by 50±1 mm. The thickness of specimens was 6.35 ± 0.41 mm. It was provided by appropriate number of plies in the specimens, whose fibers were oriented perpendicularly to flame direction (hereinafter referred to as perpendicular specimens). At least five replicates of each type of specimen were tested. The thickness of specimens with parallel-to-flame orientation of fibers (hereinafter referred to as parallel specimens) was provided by cutting. It is necessary to note that parallel specimens practically did not have flexural rigidity, thus they were additionally reinforced by gluing of metal sheets on the back-face.

Table 1. Silicon rubber composites with perpendicular orientation of plies in relation to flame direction

No	Name	Reinforcement		Specimen	
		description	superficial density, g/m^2	thickness, mm	density, g/cm^3
1	MA	fiberglass mat 450 (E-glass)	450	6.8	1.56
2	32U	unidirectional carbon tape 32U	332	6.5	1.45
3	BI52	bidirectional carbon tape BI52	200	6.4	1.46
4	110	fiberglass fabric 110 (E-glass)	110	6.6	1.58
5	200	fiberglass fabric 200 (E-glass)	200	6.4	1.64
6	300	fiberglass fabric 300 (E-glass)	300	6.5	1.72
7	600	fiberglass fabric 600 (E-glass)	600	5.9	1.65
8	TSI	silica fiber fabric TS1000	1280	6.4	1.70
9	TCE	ceramic fiber tape FC1200	1460	7.0	1.54

Table 2. Silicon rubber composites with parallel orientation of plies in relation to flame direction

No	Name	Reinforcement		Specimen	
		description	superficial density, g/m^2	thickness, mm	density, g/cm^3
10	110-II	fiberglass fabric 110 (E-glass)	110	6.4	1.48
11	200-II	fiberglass fabric 200 (E-glass)	200	6.5	1.51
12	300-II	fiberglass fabric 300 (E-glass)	300	6.4	1.46
13	32U-II	unidirectional carbon tape 32U	332	6.4	1.42
14	BI52-II	bidirectional carbon tape BI52	200	6.8	1.35

3. METHODOLOGY

The methodology described in ASTM standard (ASTM, 2008) was used as a reference, but with some alterations to attend the objectives of the study (considering availability of appropriate welding equipment on Brazilian market).

The scheme of the oxyacetylene test-bench is shown in Figure 1a. The specimen is hold by four screws equipped with silicone separators to diminish the loss of heat. The specimen holder has two positions in vertical direction. The lower position is used for installation of specimen in the holder, coupling of thermocouples in adapters and setting of neutral flame in oxyacetylene torch. For a fire testing, the holder is displaced manually to upper position and the tip of lateral thermocouple passes through the flame determining a starting point of burning time. Since the heat fluxes in low-thrust hybrid propellant motors are moderate (NUNES, 2017), the welding torch (whose characteristics are given in Table 3) adopted for the test-bench had been selected on the basis of the relatively low heat flux. The same settings were used for all tests: the length of internal cone of the neutral flame was 9 mm, the distance between front face of specimen and torch tip was 9 mm. In spite of

the fact that the test-bench could be equipped with five thermocouples (Figure 1b), the back-face temperature was measured by three K-type thermocouples Omega KMQXL-062U-6 with response time 0.3 s (diameter 1.6 mm).

The tip of the first thermocouple was installed in the center of specimen's back-face (the central point 0 mm) in such way that the axis of flame would pass through this central point. The tips of the other two thermocouples were displaced along specimen's back-face in lateral direction on distance 4 and 8 mm from the central point. To immobilize the tip of a thermocouple on the back-face of a specimen, the latter was equipped with a silicone rubber strip with 5 conducting holes spaced 4 mm apart (Figure 2a). Initial moment of burning time was determined by the thermocouple Omega KMQXL-125U-6 with response time 0.4 s (diameter 3.2 mm), whose tip was installed above the upper edge of a specimen. When the specimen holder dislocates from the lower position to upper one, the thermocouple tip passes through a flame providing an impulse of temperature rise and establishing a starting point. The data from all thermocouples were recorded by data acquisition system Lynx ADS2000.

Since the tested composites were intended to be used as a heat insulator for the low-thrust hybrid propellant motor with operation time no less than 40 s, the same period of time was accepted for the oxyacetylene ablation testing.

Mass ablation rate of specimens was calculated by formula

$$a = \frac{m_0 - m_f}{\delta\tau}, \quad (1)$$

where m_0 – initial mass of specimen, g;

m_f – mass of specimen after burning time $\delta\tau$ in seconds, g;

Figure 1. The oxyacetylene test-bench: a) the scheme; 1 – specimen holder; 2 – specimen; 3 – torch; 4 – test-bench plate; 5 – gas hose inlet; b) photo of the test-bench equipped with 5 thermocouples for back-face measurements and one lateral thermocouple for timing of burning

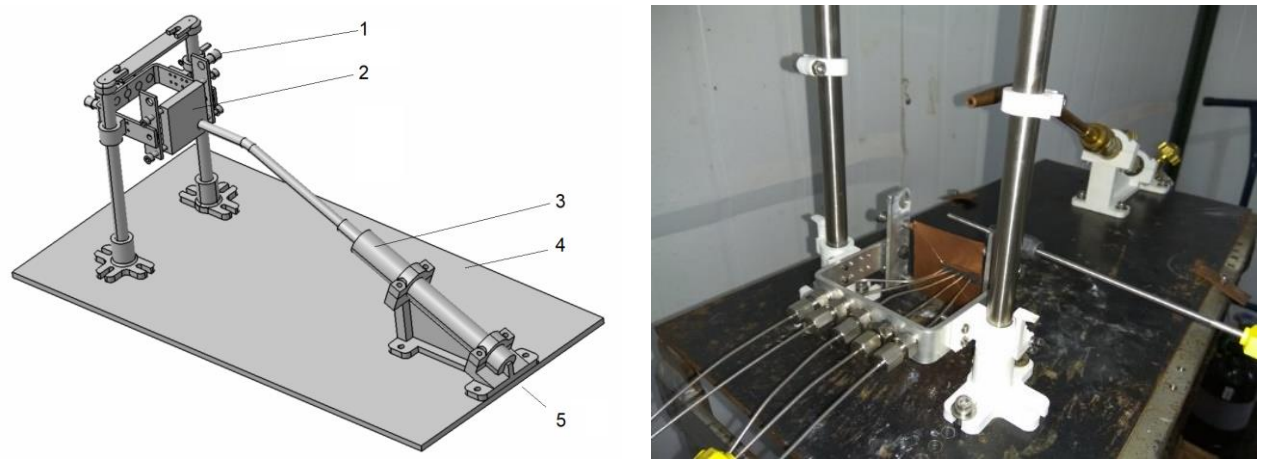

a) b)

A special specimen was prepared for determination of incident heat flux from oxyacetylene heat source. The specimen was made from a material with relatively low thermal conductivity (silicone rubber) and had a shape of a plate with 6 rectangular through holes spaced 4 mm apart (Figure 2b). Thin copper sheets with nominal thickness 0.56 mm were embedded into the holes. The specimen front-face was in the same plane as a front surface of the copper sheets, whose back surface was in contact with thermocouple tips. The temperature measured on the back surface is a result of heat transfer through the thickness of a copper with known thermal

properties. The heat transfer through silicone rubber was ignored, because of its low thermal conductivity in comparison with copper and the specimen was exposed to oxyacetylene flame for a short period of time.

Table 3. Characteristics of welding torch Condor 201 AC#9 adapted for oxyacetylene test-bench

Pressure, kgF/cm^2		Flow rate, l/h	
oxygen	acetylene	oxygen	acetylene
0.10 – 0.40	0.20 – 0.40	220 – 270	210 – 250

Heat flux in the first approximation was calculated by the heat diffusion equation for the case of unidirectional heat transfer (BARROS, 2009):

$$\dot{q_x} = \rho C_p \delta x \frac{\delta T}{\delta \tau}, \quad (2)$$

where ρ – density of copper, kg/m^3;

C_p – specific heat, J/(kg·K)

δx – sheet thickness, m;

δT – the difference between the initial temperature and the temperature after burning period $\delta \tau$ in seconds, K.

The maximum burning time $\delta \tau$ for the characterization of incident heat flux was 7 seconds.

Figure 2. The specimens used in the study: a) the typical specimen of silicone rubber composite; b) the specimen for characterization of oxyacetylene flame (back-face is on the right-hand side)

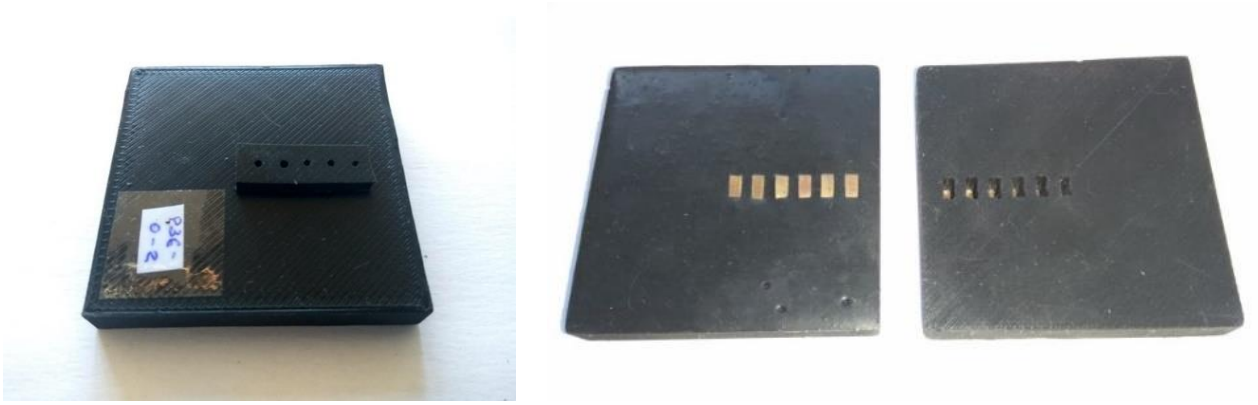

a) b)

4. RESULTS

Figure 3a shows one of the five plots of temperature vs time from oxyacetylene flame characterization tests. These data were used for calculation of heat flux by formula (2) for one of the particular coordinates of specimen and burning intervals δτ: 0 – 1 s, 0 – 2 s, 0 – 3 s, 0 – 5 s and 0 – 7 s (Figure 3b). Heat transfer from flame to specimen occurs by convection and radiation and depends on temperature of external surface of copper sheets. After observation of data on Figure 3a, it was accepted the interval 2 – 7 seconds for calculation of incident heat flux, whose mean values from 5 measurements are: 114.5±24 kW/m^2 for the central point 0 mm, 44±14.5 kW/m^2 for the central point 4 mm, 18±4.9 kW/m^2 for the central point 8 mm.

Figure 3. The results of oxyacetylene flame characterization: a) the measured back-face temperature; b) the calculated incident heat flux

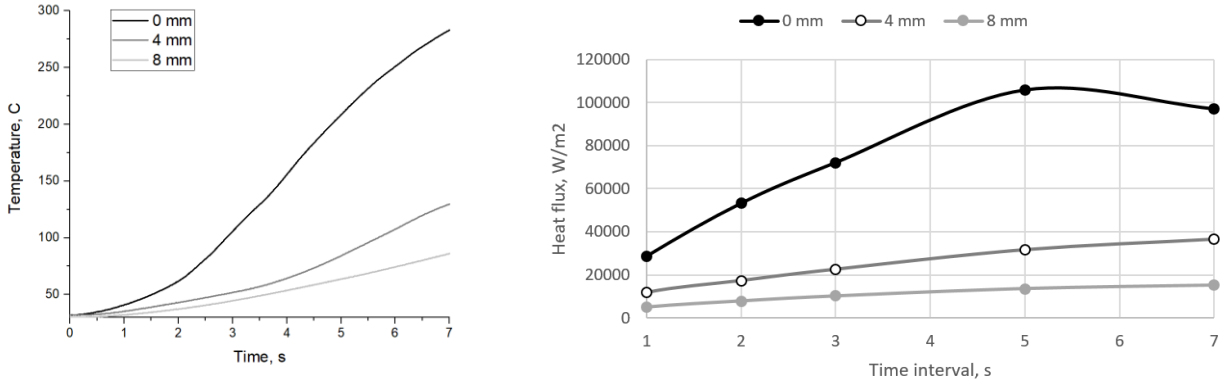

a) b)

According to the results on insulating effectiveness of the tested specimens reinforced by fibers perpendicularly to direction of oxyacetylene flame (Table 4), the maximum back-face temperature after 40 s is in the range 60 – 85°C for all tested specimens. The ranges of temperature for the points 4 and 8 mm are 50 – 70°C and 50 – 65°C respectively, that indicates practically the same insulating effectiveness of the specimens reinforced by various fibers at the given testing conditions. However, reasons of the similar effectiveness are not the same for all specimens.

Table 4. Insulating effectiveness of the silicon rubber composites

Fiber material	Type	Mean thickness, mm	Temperature after 40 s for three points of measurements, °C					
			0 mm		4 mm		8 mm	
			mean	deviation	mean	deviation	mean	deviation
E-glass	MA	6.8	58.4	1.3	51.0	2.2	50.1	1.5
	110	6.6	73.4	1.0	58.5	2.3	54.2	2.5
	200	6.4	72.0	3.5	60.7	6.6	50.9	0.3
	300	6.5	66.4	1.9	53.9	3.2	55	2.7
	600	5.9	85.8	0.5	70.3	1.8	65.6	4.2
carbon	32U	6.5	67.5	3.7	61.3	4.3	59.8	6.3
	BI52	6.4	74.4	8.1	65.8	6.6	63.6	7.1
silica	TSI	7.0	72.9	5.4	62.0	3.0	60.4	2.3
ceramic	TCE	6.5	79.0	2.3	67.3	4.9	63.9	5.0

It is known that axial thermal conductivity for E-glass fiber is one order less than for a standard-modulus polyacrylonitrile carbon fiber (ZWEBEN, 2006). At the same time, the depth of crater in fiberglass specimens is greater than in carbon or ceramic fiber specimens (Figure 4). The specimens reinforced by glass and carbon fibers (Figures 4a and 4d respectively) were subjected to flame for 58 s. As a result, the former specimen have suffered dilatation and the minimal measured thickness through the bottom of the crater was 5.4 mm. At the same time, the latter specimen did not swell and the minimal residual thickness was 6.4 mm. Therefore, for the given testing conditions, lower thermal conductivity of fiberglass specimens is compensated by small residual thickness, and for carbon fiber specimens, higher thermal conductivity is compensated by greater residual thickness.

Figure 4. The cross-sections through the center of tested silicon rubber specimens: a) fiberglass 110 (burning time $\Delta\tau$ = 58 s); b) fiberglass 600 ($\Delta\tau$ = 41 s); c) fiberglass 300 ($\Delta\tau$ = 41 s); d) carbon fiber 32U ($\Delta\tau$ = 58 s); e) ceramic fiber TCE ($\Delta\tau$ = 41 s); f) silica fiber TSI ($\Delta\tau$ = 41 s)

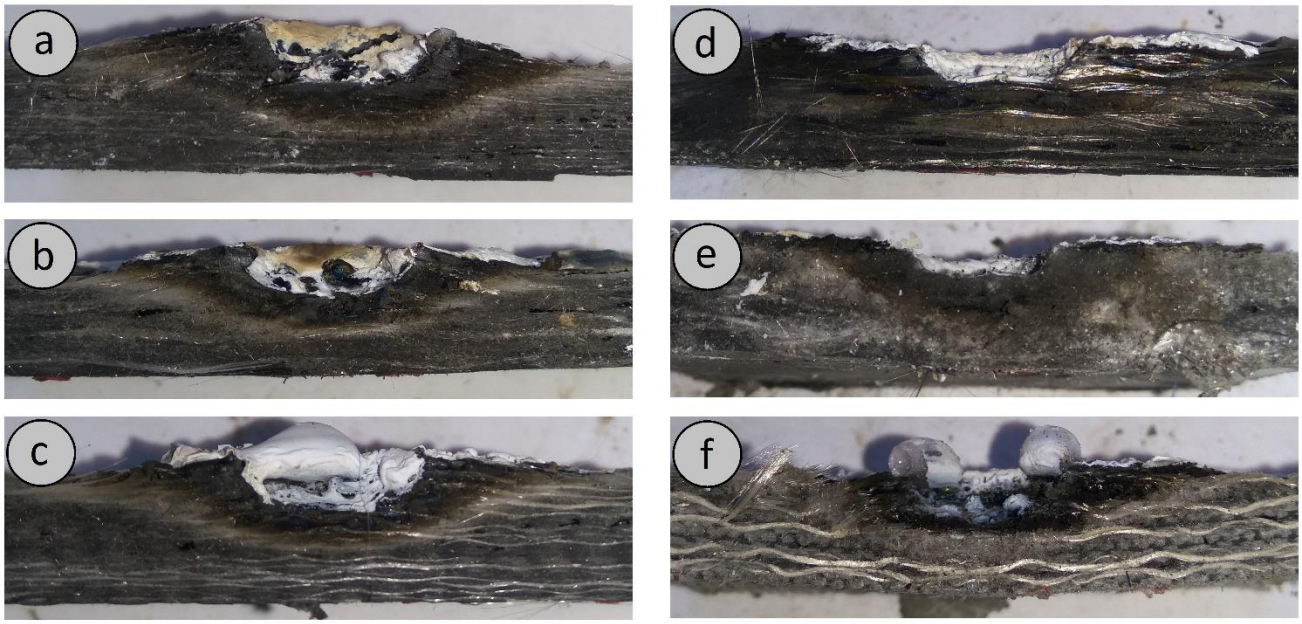

It is necessary to note that ablation rate by mass is lower for fiberglass specimens (Table 5). It can be explained by the effect of full reflection of flame from the front surface of specimen when the crater in specimen takes the form of semi-ellipsoid. In the carbon fiber specimens, such shape of crater does not form (Figure 4d) and the flame is distributed over the front face of specimen (Figure 5a). The burning occurs over all front face of specimen and the mass losses are higher. Half of the specimens reinforced with ceramic tape did not have the effect of flame reflection and the shape of crater does not look like profound hemi-ellipsoid (Figure 4e). In most of the specimens, the full reflection of flame (Figure 5c) occurs after some time, which is difficult to determine accurately due to transition effect (Figure 5b).

Table 5. Ablation rates of the tested silicon rubber composites

Fiber material	Type	Mean thickness, mm	Ablation rate for 40 s, g/s		Full flame reflection time, s	
			mean	deviation	mean	deviation
glass	MA	6.8	0.017	0.001	24.9	3.8
	110	6.6	0.017	0.003	28.7	11.2
	200	6.4	0.015	0.002	20.3	4.0
	300	6.5	0.013	0.003	25.1	3.8
	600	5.9	0.015	0.002	28.5	5.9
carbon	32U	6.5	0.027	0.003	-	-
	BI52	6.4	0.027	0.008	-	-
silica	TSI	6.4	0.013	0.003	29.2	0.2
ceramic	TCE	7.0	0.025	0.002	30.3*	0.3*

* data for 2 specimens only

Due to full reflection, some specimens lose their mass just over some restricted area of a formed crater, which leads to lower mass loss along the established burning time. It is expected that in case of prolongation of burning time, ablation rate of the specimens susceptible to flame reflection has to increase.

Figure 5. The effect of flame reflection for the same specimen MA: a) no flame reflection; b) partial reflection of flame; c) full reflection of flame

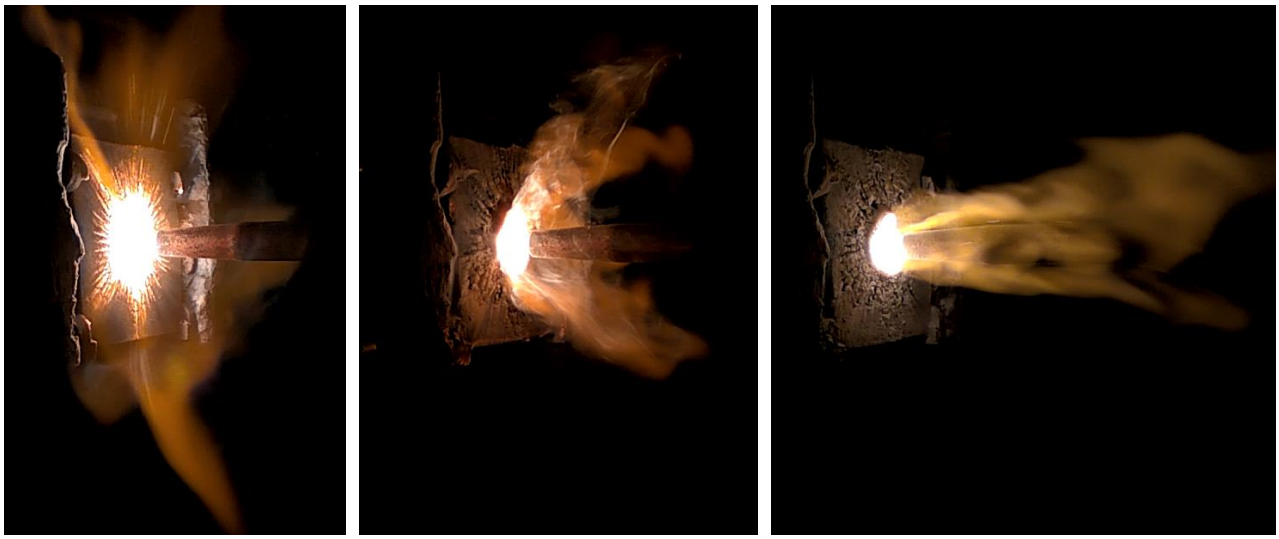

a) b) c)

Figure 6 shows data on temperature measurement on the back-face of specimens, whose fibers have parallel or perpendicular orientation in relation to flame direction. According to the data in Figure 6, the temperature in the specimens, whose fibers have parallel orientation in relation to flame direction (marked with "-11-"), increases much faster than in specimens with perpendicular orientation of fibers. In the parallel specimens reinforced by fabric, at least half of the fibers is arranged along the thickness of specimen. This portion of fibers serves as a heat conductor, since heat propagates easily along the length of the fibers. As thicker is a fiberglass fabric, as better it conducts a heat in parallel specimens: the temperature on back-face of the specimens 300 is growing faster than on back-face of the specimens 110 and 200 (Figure 6a). The temperature rises faster in specimens with parallel orientation of carbon fibers than in fiberglass specimens with the same orientation due to higher heat conductivity of carbon (Figure 6b).

For parallel specimens reinforced with carbon fibers, burning time was reduced to 30 s. In case of burning time above 30 s, these specimens start to deflect due to low flexural rigidity and thermocouples escape from their previous positions. Carbon fibers oriented along the thickness of ablator demonstrate increased resistance to erosion because of high melting temperature of carbon and the roots of the fibers are held by non-heated matrix. After 30 s of burning, there are no sign of thickness reduction in specimens reinforced by carbon fibers in comparison to fiberglass specimens (Figure 7). High thermal conductivity of carbon is not compensated anymore by greater thickness like in specimens with perpendicular orientation of fibers, therefore the temperature on the back-face of parallel specimens grows faster (Figure 6a).

In perpendicular specimens, there are no fibers oriented along the thickness. The heat from front-face to back-face of specimen propagates through the thickness of fibers and silicone rubber. Since heat conductivity for silicone rubber is lower than for fibers, the temperature growth is slower for specimens with perpendicular orientation of fibers. It explains the least temperature in perpendicular specimen MA reinforced by fiberglass mat (Figure 6a). Here, fibers are distributed arbitrary in various directions in the plane of ply, which is perpendicular to flame direction.

Figure 6. Temperature measurements on back-face central point 0 mm of the selected specimens reinforced by fiberglass (a) and carbon (b) fibers with parallel (blue curves) and perpendicular (green curves) orientation in relation to flame direction

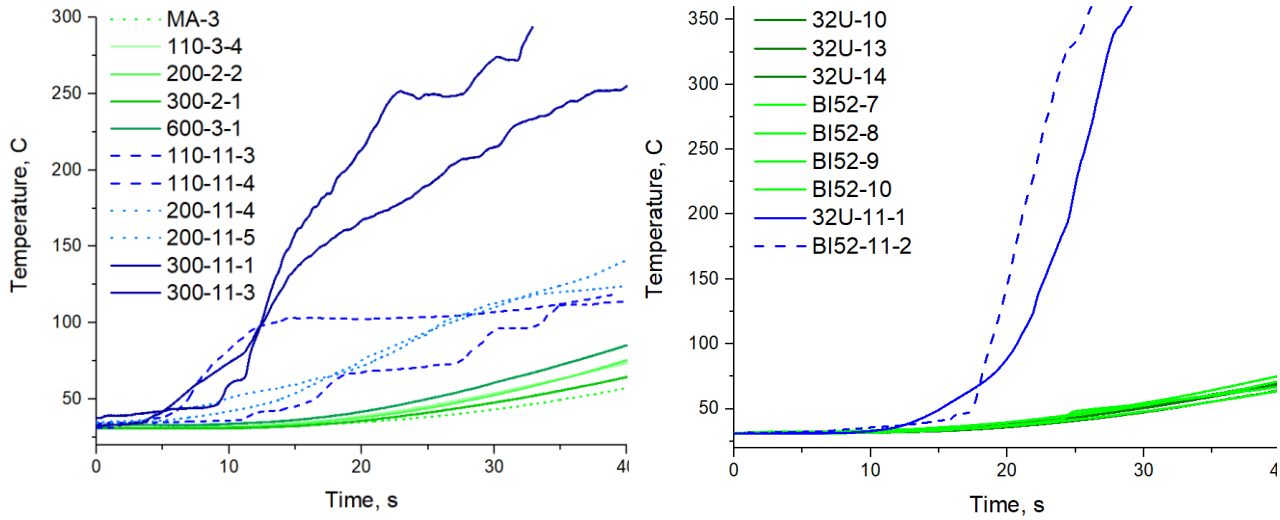

a) b)

Figure 7. The cross-sections through the center of tested specimens with parallel orientation of fibers in relation to flame direction: a) 32U-11 (burning time $\Delta\tau$ = 30 s); b) fiberglass 200-11 ($\Delta\tau$ = 30 s)

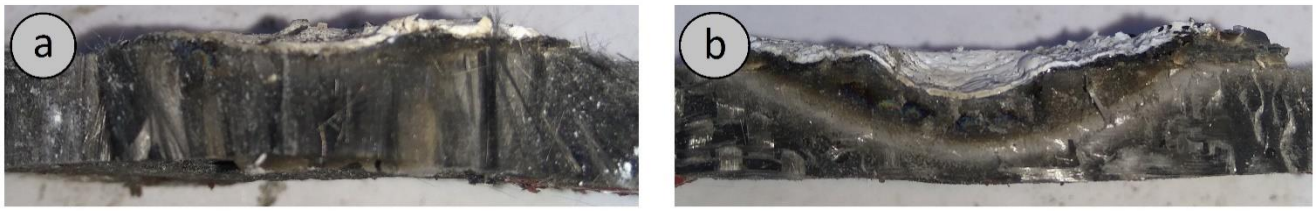

5. CONCLUSIONS

The reinforcement of silicone rubber composites with fiberglass fabric or carbon tape in parallel-to-flame direction is impractical due to low insulating effectiveness. After 40 s of burning, the back-face temperature of perpendicular specimens reinforced by E-glass is in the range 58.4 – 85.8°C, while in parallel specimens it exceeds 100°C. For carbon-reinforced composites, this difference is even greater due to high thermal conductivity of carbon: the back-face temperature of perpendicular specimens is in the range 67.5 – 74.4°C after 40 s of burning, whereas in parallel specimens the temperature is greater than 350°C after 30 s of burning.

The comparison of mass ablation rate of parallel specimens was prejudiced by the effect of flame reflection that was observed after 20 – 30 s of burning in all composites except those reinforced with carbon and ceramic fibers. The latter specimens had higher mass ablation rate 0.025 - 0.027 g/s than fiberglass and silica specimens, whose mass ablation rate was in the range 0.013 – 0.017 g/s.

For the given conditions of tests (heat flux from the oxyacetylene torch 114.5±24 kW/m^2 and burning time 40 s), the tested silicone rubber composites reinforced with E-glass, carbon, silica and ceramic fabrics (or tapes) with perpendicular orientation of plies in relation to flame direction demonstrated almost the same insulation effectiveness. The least back-face temperature 58.4±1.3°C was observed in specimens MA reinforced with fiberglass mat (density 1.56 g/cm^3); however, the mean thickness of these specimens was

slightly higher than in other specimens except those reinforced by ceramic fibers. In spite the fact that the back-face temperature 67.5±3.7°C of specimens reinforced by carbon tape 32U was higher than in MA specimens, their principal advantage is the least mean density 1.45 g/cm^3.

It is evident that for low-cost systems, like low-thrust hybrid propulsion rocket motors with relatively short operation time, the less expensive fiberglass composites could be applied for fabrication of internal insulation with insignificant losses in efficiency. However, their efficiency has to be confirmed experimentally in conditions of hybrid propellant rocket motor.

6. ACKNOWLEDGEMENTS

The authors acknowledge the Foundation of Research Projects in Federal District (FAP DF) for financial support of the study.

7. REFERENCES

AHMED, A.F. **Thermal insulation by heat resistant polymers**. Montreal: Concordia University, 2009.

ANDRIANOV, A.; SHYNKARENKO, O. ; BERTOLDI; A.E.M. ; BARCELOS, JR., M.N.D. ; VERAS, C.A.V. Concept and design of the hybrid test-motor for development of a propulsive decelerator of SARA re-entry capsule. In: AIAA/SAE/ASEE JOINT PROPULSION CONFERENCE, 51., 2015. **Anais eletrônicos...** Orlando: AIAA, 2015. Disponível em: <https://arc.aiaa.org/doi/10.2514/6.2015-3941>. Acesso em: 23 set. 2018.

AMERICAN SOCIETY FOR TESTING AND MATERIALS. **ASTM E285 – 08**: Standard test method for oxyacetylene ablation testing of thermal insulation materials. West Conshohocken, 2008.

BARROS, E.A.; FILHO, G.P.; GREGORI, M.L.; COSTA E SILVA, S.F.; CHARAKHOVSKI, L.I.; MACIEL, H.S. Thermal response and ablation characteristics of quartz-phenolic and carbon-phenolic composites. In: INTERNATIONAL CONGRESS OF MECHANICAL ENGINEERING, 20., 2009. **Anais eletrônicos...** Gramado: ABCM, 2009. Disponível em: <http://www.abcm.org.br/anais/cobem/2009/pdf/COB09-1392.pdf>. Acesso em: 23 set. 2018.

CHAPMAN, A.J. **Evaluation of several silicone, phenolic, and epoxy base heat-shield materials at various heat transfer rates and dynamic pressures**. Washington, D.C.: NASA, 1966.

DONSKOY, A. Elastomeric heat-shielding materials for internal surfaces of missile engines. **International journal of polymeric materials and polymeric biomaterials**, v. 31, n. 1-4, p. 215-236, 1996.

FAVALORO, M. Ablation materials. In: **Kirk-Othmer Encyclopedia of Chemical Technology**. John Wiley & Sons Inc., 1998. p. 1-8.

KIM, E.S.; KIM, E.J.; SHIM, J.H.; YOON, J.S. Thermal stability and ablation properties of silicone rubber composites. **Journal of Applied Polymer Science**, v. 110, n. 2, p.1263-1270, 2008.

KIM, E.S.; LEE, T.H.; SHIN, S.H.; YOON, J.S. Effect of incorporation of carbon fiber and silicon carbide powder into silicone rubber on the ablation and mechanical properties of the silicone rubber-based ablation material. **Journal of Applied Polymer Science**, v. 120, n. 2, p. 831-838, 2011.

KOO, J.H., MILLER, M.J., WEISPFENNING, J., BLACKMON, C. Silicone polymer composites for thermal protection system: fiber reinforcements and microstructures. **Journal of composite materials**, v. 45, n. 13, p. 1363-1380, 2011.

MAZETTI, A.; MEROTTO, L.; PINARELLO, G. Paraffin-based hybrid rocket engines applications: A review and a market perspective. **Acta Astronautica**, v. 126, p. 286-297, 2016.

MILHOMEM, G.; NUNES, A. P.; ANDRIANOV, A.; SHYNKARENKO O.; LEE, J. In: ABCM INTERNATIONAL CONGRESS OF MECHANICAL ENGINEERING, 24., 2017. **Anais eletrônicos...** Curitiba: ABCM, 2017. Disponível em: <http://www.sistema.abcm.org.br/articleFiles/download/11953>. Acesso em: 23 set. 2018.

MILLER, M.J.; KOO, J.H.; WILSON, D; BECKLEY, D.A. Effect of reinforcements in a silicone resin composite. In: AIAA AEROSPACE SCIENCES MEETING, 32., 1994. **Anais eletrônicos...** Reno: AIAA, 1994. Disponível em: <https://arc.aiaa.org/doi/10.2514/6.1994-787>. Acesso em: 23 set. 2018.

THE NATIONAL AERONAUTICS AND SPACE ADMINISTRATION. **NASA SP-8093:** Solid rocket motor internal insulation. NASA-Langley, 1977. 116 p.

NATALI, M.; KENNY, J.M.; TORRE, L. Science and technology of polymeric ablative materials for thermal protection systems and propulsion devices: A review. **Progress in Material Science**, v. 84, p. 192-275, 2016.

NUNES, A.P.C.P.; MILHOMEM, G.P.; RISPOLI, V.C.; ANDRIANOV, A. Application of an inverse method for the estimation of heat flux in low-thrust hybrid propellant rocket motor. In: PROCEEDINGS OF THE XXXVIII IBERIAN LATIN-AMERICAN CONGRESS ON COMPUTATIONAL METHODS IN ENGINEERING, 38., 2017. **Anais eletrônicos...** Florianópolis: CILAMCE, 2017. Disponível em: <https://ssl4799.websiteseguro.com/swge5/PROCEEDINGS/PDF/CILAMCE2017-0107.pdf >. Acesso em: 23 set. 2018.

OYUMI, Y. Ablation characteristics of silicone insulation. **Journal of Polymer Science Part A: Polymer Chemistry**, v. 36, n. 2, p. 233-239, 1998.

SCHMIDT, D.L. **Ablative plastics and elastomers in chemical propulsion environments.** Wright-Patterson Air Force Base, Ohio: Air Force Materials Laboratory, Research and Technology Division, Air Force Systems Command, 1965. 123 p.

SCHMIDT, D.L. Ablative polymers in aerospace technology. **Journal of Macromolecular Science: Part A – Chemistry**, v. 3, n. 3, p. 327-365, 1969.

YANG, D.; ZHANG, W.; JIANG, B. Ceramization and oxidation behaviors of silicone rubber ablative composite under oxyacetylene flame. **Ceramics International**, n. 39, p. 1575-1581, 2013a.

YANG, D.; ZHANG, W.; JIANG, B.; GUO, Y. Silicone rubber ablative composites improved with zirconium carbide or zirconia. **Composites Part A**, v. 44, p. 70-77, 2013b.

YOUREN, J.W. Ablation of elastomeric composites for rocket motor insulation. **Composites**, v. 2, n. 3, p.180-184, 1971.

YU, L.; ZHOU, S.; ZOU, H.i; LIANG, M. Thermal stability and ablation properties study of aluminum silicate ceramic fiber and acicular wollastonite filled silicone rubber composite. **Journal of Applied Polymer Science**, v. 131, n. 1, 2014.

ZHANG, G.; WANG, F.; HUANG, Z.; DAI, J.; SHI, M. Improved Ablation Resistance of Silicone Rubber Composites by Introducing Montmorillonite and Silicon Carbide Whisker. **Materials**, v.9, n. 9, p. 723, 2016.

ZHOU, W.; YANG, H.; GUO, X.; LU, J. Thermal degradation behaviors of some branched and linear polysiloxanes. **Polymer Degradation and Stability**, v. 91, n. 7, p. 1471-1475, 2006.

ZHOU, C.; YU, L.; LUO, W.; CHEN, Y.; ZOU, H.; LIANG, M. Ablation properties of aluminum silicate ceramic fibers and calcium carbonate filled silicone rubber composites. **Journal of Applied Polymer Science**, v. 132, n. 11, p. 41619, 2015.

ZWEBEN, C. Composite materials. In: **Mechanical Engineers' Handbook (Third Edition). Materials and Mechanical Design.** John Wiley & Sons, Inc., 2006. p. 380-417.